Theoretical Determination of Molecular Structure and Conformation. 19. Configurational Changes of Bridged Annulenes: Inversion at an Ether Oxygen Atom

Dieter Cremer,*[1a] Elfi Kraka,[1a] Jürgen Gauss,[1a] and Charles W. Bock[1b]

Contribution from the Institut für Organische Chemie, Universität Köln, D-5000 Köln 41, West Germany, and the Department of Chemistry, Philadelphia College of Textiles & Science, Philadelphia, Pennsylvania 19144. *Received December 27, 1985*

Abstract: The configurational stability of oxido-bridged [10]annulenes and [14]annulenes has been investigated by HF/STO-3G, HF/4-31G, MP2/STO-3G, MNDO, and correlation-corrected MNDO calculations. It is shown that bridge inversion occurs when heating 1,6:8,13-bisoxido[14]annulene (**13**). The calculated barrier of 32–34 kcal/mol is in accord with the barrier to racemization (32 kcal/mol) of an optically active derivative of **13**. Bridge inversion is essentially an inversion at an ether oxygen, the first which has been observed so far. The barrier to bridge inversion can be reduced by widening the annulene perimeter. Barrier values of 29 and 27 kcal/mol are predicted for 1,6-imino-8,13-oxido[14]annulene (**21**) and 1,6-methano-8,13-oxido[14]annulene (**24**). An experimental verification for these predictions is suggested.

Inversion about pyramidal nitrogen is a well-established phenomenon.[2] Some experimental data are also available describing the inversion of a tricoordinate oxygen with pyramidal geometry.[3] There are, however, no direct experimental observations with regard to an inversion at a dicoordinate ether oxygen (**1a** → **2** → **1b**).

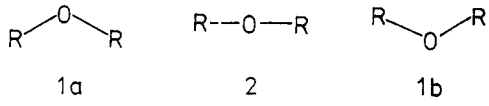

1a 2 1b

The inversion **1a** → **1b** leads to transition state (TS) **2**, with a linear arrangement of CO bonds causing rehybridization at the O atom and, thus, a transfer of its electron lone pairs from sp^n ($n \approx 3$) hybrid orbitals into high-lying $p\pi$ orbitals. As a consequence, the inversion process requires a relatively high activation energy. Ab initio calculations on H_2O[4] suggest a barrier of 37 kcal/mol. This value is considerably increased (decreased) if an electron donor (acceptor) is directly bonded to the O atom, thus (de)populating the $2p\pi$ (O) obitals.[5,6]

Experimental detection of inversion at an ether O atom will only be possible if two basic requirements are fulfilled. First, inversion has to be energetically more favorable than rotation at the CO bonds. Second, the physical and chemical properties of the ether forms **1a** and **1b** must differ in order to detect inversion about the ether oxygen.

Normally rotation at the CO bond is a rather low-energy process requiring 1–3 kcal/mol.[7] The barrier for rotation, however, will increase if the CO bond attains some double bond character as in alkoxycarbenium ions, $YCHOR^+$ (Scheme I). Both theoretical and experimental investigations suggest that ions like $CH_2OCH_3^+$ or $CH_3CHOCH_3^+$ stereomutate in the gaseous phase by inversion at the O atom, while in solution phase rotation at the CO bond is more likely.[6] If electronic effects lead to a further increase of the rotational barrier, inversion at O will eventually become the dominant process in both media.[6b]

Apart from the electronic effects, steric effects may also prevent rotation at a CO bond. If, for example, the ether group is positioned inside a fairly rigid ring framework, which possesses roughly rectangular shape (compare with Scheme I), then inversion at O will be more likely than rotation at the CO bond upon heating of the compound. In practice, synthesis of such compounds should be difficult, since it requires the formation of an accurate-scale ring template according to the bulk of the group OR (Scheme I).

Scheme I

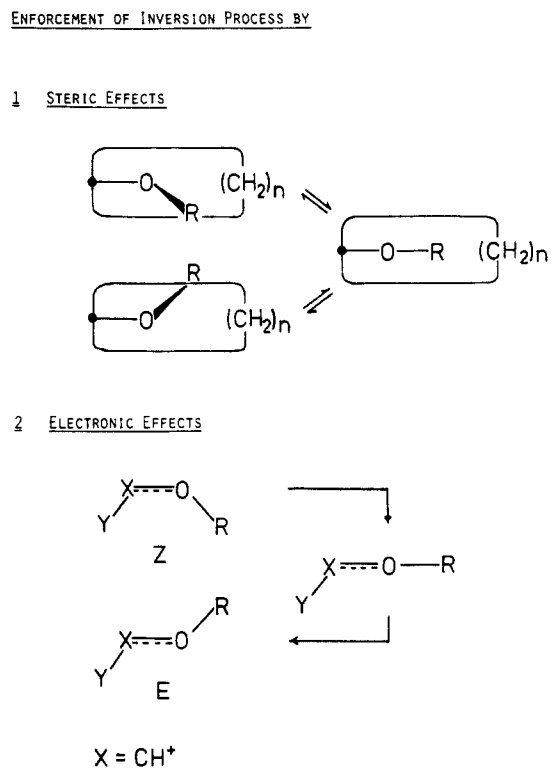

The problem of adjusting the dimensions of the ring framework to the size of the ether group will be facilitated if both oxygen valences are linked to ring atoms, thus forming an oxido-bridged ring (**3**) as is schematically shown in Scheme II. Provided that $X \neq Y$ in **3**, then compound **3** is chiral and the two enantiomers **3a** and **3b** exist. Interconversion of these enantiomers is possible either via path A or via path B (Scheme II). In the first case, the O atom swings through the center of the ring, i.e., the molecule traverses TS **4** (Scheme II) characterized by a linear arrangement of CO bonds (inversion at O). In the second case, the O bridge buckles sidewards into and through the ring (TS **5**, Scheme II).

(1) (a) Universität Köln. (b) Philadelphia College of Textiles & Science.
(2) Lehn, J. M. *Top. Curr. Chem.* **1970**, *15*, 311–377.
(3) (a) Lambert, J. B.; Johnson, D. H. *J. Am. Chem. Soc.* **1968**, *90*, 1349–1350. (b) Brownstein, S. *J. Am. Chem. Soc.* **1976**, *98*, 2663–2664.
(4) Cremer, D. *J. Am. Chem. Soc.* **1979**, *101*, 7199–7205.
(5) Cremer, D. In *The Chemistry of Functional Groups, Peroxides*; by Patai, S., Ed.; Wiley: New York, 1983; pp 1–84.
(6) (a) Cremer, D.; Gauss, J.; Childs, R. F.; Blackburn, C.; *J. Am. Chem. Soc.* **1985**, *107*, 2435–2441. (b) Blackburn, C.; Childs, R. F.; Cremer, D.; Gauss, J. *J. Am. Chem. Soc.* **1985**, *107*, 2442–2448.
(7) (a) Ivash, E. V.; Dennison, D. M. *J. Chem. Phys.* **1964**, *40*, 2109–2114. (b) Cremer, D.; Binkley, J. S.; Pople, J. A.; Hehre, W. J. *J. Am. Chem. Soc.* **1974**, *96*, 6900–6903.

0002-7863/86/1508-4768$01.50/0

Scheme II

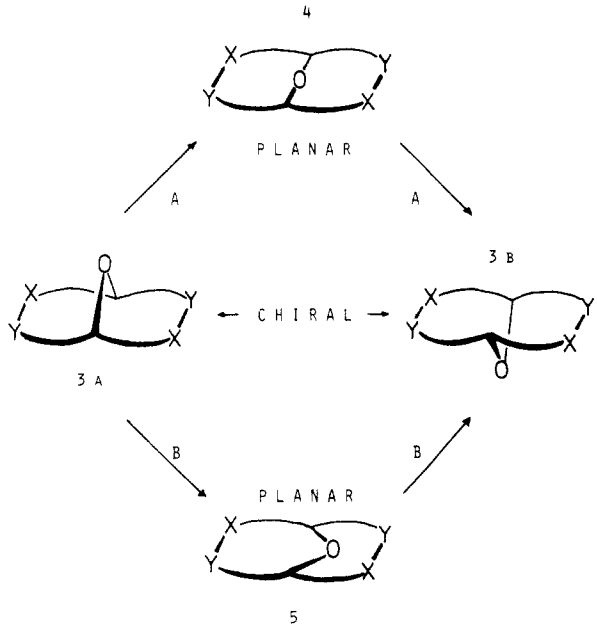

This process comprises partial rotations at the CO bonds typical of the inversion of a ring through its planar form. Thus, one may call this process a "ring inversion".

If one is able to isolate an optically active form **3a** (**3b**), then it will be possible to determine the rate of bridge inversion by measuring the rate of racemization. This rate will critically depend on the diameter of the ring, i.e., the nature of X and Y. However, it will not be possible to distinguish whether bridge inversion proceeds via path A or via path B.

Suitable candidates for compounds **3** have been synthesized by Vogel and co-workers in the form of oxido-bridged annulenes with 10π (**6**) and 14π perimeter (**7**).[8] Racemization of optically active

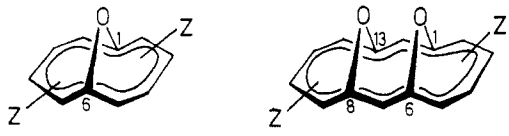

6 7

2,9-dibromo-*syn*-1,6:8,13-bisoxido[14]annulene (Z = Br) has been observed and a preliminary rationalization of the experimental results has been reported.[9]

Prompted by these observations, we felt that a more detailed investigation on the configurational stability of oxido-bridged annulenes was needed. In this work, we report the results of both semiempirical and ab initio calculations carried out for the oxido-bridged annulenes shown in Figure 1, namely 1,6-oxido[10]annulene (**8**), *syn*-1,6:8,13-bisoxido[14]annulene (**13**), *syn*-1,6-imino-8,13-oxido[14]annulene (**21**), and *syn*-1,6-methano-8,13-oxido[14]annulene (**24**). On the basis of these calculations we will discuss the following questions. (1) What are the geometrical prerequisites for observing bridge inversion? (2) How do electronic effects and/or steric effects influence bridge inversion? (3) Does the interconversion process occur by inversion at the O atom (path A) or by ring inversion (path B, scheme II)? (4) What does the mechanism of the racemization of type **7** compounds look like? (5) Is it likely that bridge inversion also occurs for other bridged annulenes?

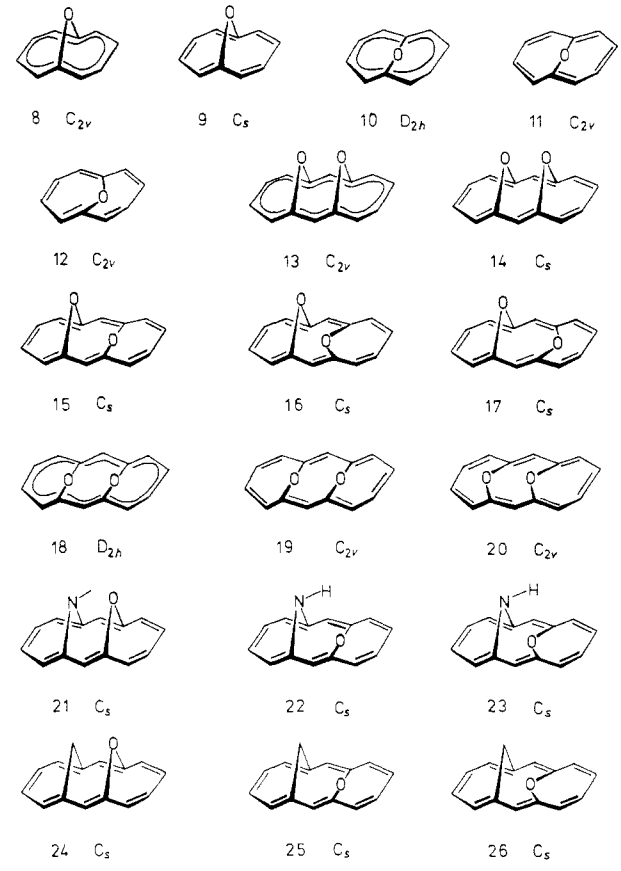

Figure 1. Annulene structures **8**–**26**. Primed structures (**12′**, **15′**, **16′**, etc.) which can be derived from the unprimed structures by a double bond shift are not shown. In the case of **21**–**23** only the forms with an endo oriented NH bond are depicted.

Table I. Relative Energies and Heats of Formation $\Delta H_f°$ ($\Delta\Delta H_f°$) of Delocalized and Localized Structures of Oxido-Bridged Annulenes[a]

method	**8** (C_{2v})	**9** (C_s)	**13** (C_{2v})	**14** (C_s)
HF/STO-3G[b]	0	−4.3	0	−23.7
HF/4-31G	0	−0.4	0	−18.3
MP2/STO-3G	0	0.7		
MNDO	50.8	45.7	64.5	47.3
	(0)	(−5.1)	(0)	(−17.2)
MNDO/BW	61.3	62.5	90.5	84.7
	(0)	(1.2)	(0)	(−5.8)
MNDO/BW + size consistency correction[c]	46.0 (0)	50.4 (4.4)	63.2 (0)	65.5 (2.3)
exptl[d]	47.8 ± 1.2			

[a] All values in kcal/mol. HF energies have been evaluated at MNDO geometries. STO-3G: −452.399 67 (**8**), −676.951 75 (**13**). HF/4-31G: −457.428 28 (**8**), −684.515 08 (**13**). MP2/STO-3G: −453.047 34 hartree (**8**). [b] Geometry optimization of **13** and **14** at the HF/STO-3G level lead to −676.981 71 hartree for **13** and a relative energy of −20.2 kcal/mol for **14**. [c] Reference 12b. [d] Reference 19.

Quantum Chemical Methods

In this work both semiempirical MNDO[10] and nonempirical Hartree–Fock (HF) calculations have been carried out. MNDO has been used to obtain equilibrium geometries and heats of formation, $\Delta H_f°$, of the annulene forms shown in Figure 1. Since MNDO as other NDO approaches has a tendency of underestimating electron delocalization, thus favoring annulene structures with strongly alternating bonds,[27] calculations have been repeated at the correlation corrected level of MNDO theory using second-order Brillouin–Wigner (BW) perturbation theory, which is comparable to considering all doubly excited configurations.[11] It turned out that due to the size consistency error of the

(8) Vogel, E.; Giskup, M.; Pretzer, W.; Böll. W. A. *Angew. Chem.* **1964**, *76*, 785; *Angew. Chem., Int. Ed. Engl.* **1964**, *3*, 642. Sondheimer, F.; Shani, A. *J. Am. Chem. Soc.* **1964**, *86*, 3168–3169. Vogel E.; Biskup, M.; Vogel, A.; Günther, H. *Angew. Chem.* **1966**, *78*, 755–756; *Angew. Chem., Int. Ed. Engl.* **1966**, *5*, 734. Vogel, E. *Chimia* **1968**, *22*, 21–32.

(9) (a) Vogel, E.; Tückmantel, W.; Schlögl, K.; Widhalm, M.; Kraka, E.; Cremer, D. *Tetrahedron Lett.* **1984**, *25*, 4925–4928. (b) Scharf, J.; Schlögl, K.; Widhalm, M.; Lex, J.; Tückmantel, W.; Vogel, E.; Pertlik, F. *Monatsh. Chem.* **1986**, *117*, 255–267. (c) Tückmantel, W. Ph.D. Thesis, Cologne, 1984.

(10) Dewar, M. J. S.; Thiel, W. *J. Am. Chem. Soc.* **1977**, *99*, 4899–4907.

(11) Thiel, W. *J. Am. Chem. Soc.* **1981**, *103*, 1413–1420, 1420–1425.

Table II. Theoretical and Experimental Geometries of 1,6-Oxido[10]annulene and 1,6:8,13-Bisoxido[14]annulene[a]

	8		9		13		14		27	
parameter[b]	MNDO	exptl[c]	MNDO	STO-3G	MNDO	exptl[d]	STO-3G	MNDO	STO-3G	MNDO
$R(1,6)$	2.209	2.22	2.216	1.921	2.277	2.249	2.258	2.306	2.314	2.346
							2.299	2.331	2.360	2.374
$R(1,2)$	1.423	1.39	1.424	1.482	1.439	1.394	1.337	1.373	1.326	1.364
			1.422				1.489	1.476	1.491	1.476
$R(2,3)$	1.399	1.39	1.397	1.330	1.384	1.385	1.469	1.461	1.482	1.464
			1.401				1.328	1.359	1.326	1.357
$R(3,4)$	1.419	1.39	1.420	1.466	1.429	1.402	1.338	1.364	1.330	1.361
			1.418				1.487	1.464	1.489	1.464
$R(6,7)$				1.393	1.413	1.392	1.485	1.475	1.510	1.486
							1.333	1.370	1.326	1.370
$R(C,O)$	1.388	1.43	1.386	1.422	1.385	1.396	1.420	1.387	1.423	1.387
							1.416	1.382	1.414	1.383
$R(O,O)$				2.562	2.605	2.550	2.463	2.572	2.941	2.865
$\angle 1,2,3$	123.5		123.2	123.9	124.7	123.7	122.3	123.8	122.9	124.4
			123.3				124.1	124.7	124.8	125.5
$\angle 2,3,4$	127.0		127.3	124.8	127.9	127.1	125.1	125.8	125.4	126.0
			127.2				129.0	128.8	129.3	128.9
$\angle 6,7,8$				123.0	125.4	125.0	122.1	124.8	117.9	120.9
$\angle OCC$	114.8		114.8	115.9	115.0	114.5	117.7	117.1	119.4	119.9
			114.8				113.7	113.3	115.9	115.2
$\angle OCC$				119.8	118.6	118.6	116.3	115.9	112.6	110.8
							120.5	119.6	116.8	116.3
$\angle COC$	105.5	102	106.1	85.0	110.5	107.8	105.3	112.5	108.7	115.4
							108.5	115.0	113.3	118.3
τ_1	13.5		13.3	6.4	4.6	19.2	30.7	26.0	30.4	25.6
			13.5				5.9	0.4	4.9	0.2
τ_2	146.9		146.8	145.2	145.1	156.4	164.9	162.3	171.2	168.6
			147.0				147.2	144.4	154.3	149.9
τ_3				175.8	163.7	166.7	165.8	159.0	118.2	123.9
							169.3	162.6	171.8	166.9

[a] Distances in Å, angles in deg. [b] In the case of C_s symmetrical forms, geometrical parameters which correspond to each other are given in one row. The first OCC angle corresponds to OC1C2. The dihedral angles τ of the annulene perimeter are defined as

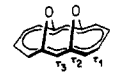

[c] Reference 17. Only averaged CC bond lengths are given. [d] Reference 18.

MNDO/BW approach, correction of calculated $\Delta H_f°$ values by formulas given by Davidson[12a] and Pople and co-workers[12b] was essential to obtain the correct energy minima of the parent annulenes (see Table I). Since Pople's formula explicitly depends on the number of electrons, it leads to better correlation corrections in the case of large molecules containing delocalized π-systems.[13]

As for a consistent description of annulene forms with alternating bond lengths (see Figure 1), test calculations indicated that MNDO is sufficient. Geometries calculated with MNDO and MNDO/BW parameters differed only slightly, leading to changes in $\Delta\Delta H_f°$ of less than 1 kcal/mol. Therefore, MNDO was used throughout this work.[28]

Various attempts have been made to verify MNDO results by ab initio calculations. Recalculation of energy differences at the HF/STO-3G and HF/4-31G levels of theory[14] utilizing MNDO geometries lead to qualitatively similar results as obtained at the semiempirical level. The STO-3G description of delocalized π-systems turns out to be inferior to the description provided by MNDO. This becomes even more apparent when the geometries of **13** and **14** were reoptimized at the HF/STO-3G level (Table II). For example, the 1,6 and 8,13 distances in **13** are reduced to the unrealistic value of 1.9 Å due to the fact that STO-3G, as other minimal basis sets, artificially favors structures with three-membered rings at the expense of their olefinic counterparts.[15] Consideration of correlation effects by second-order Møller–Plesset perturbation theory,[16] and/or an extension of the basis set improves the description (Table I). Unfortunately, complete optimization at, e.g., the the MP2/4-31G level of theory was not economically feasible. Therefore, we refrained from carrying out ab initio calculations for all structures shown in Figure 1.

Calculation of the geometries of **13–26** at the MNDO level implied the optimization of 40–50 parameters, utilizing the symmetry constraints given in Figure 1. In those cases in which the actual movement of the oxygen atom during bridge inversion was analyzed, the distance between O and the midpoint of C1,C6 was used as the reaction coordinate λ and all parameters were optimized for each fixed value of λ.

Results and Discussion

In Table I, ab initio energies and MNDO heats of formation of structures **8**, **9**, **13**, and **14** are listed. The corresponding geometries are shown in Table II. Table III contains theoretical $\Delta H_f°$ values of all structures relevant to the investigation of bridge inversion in oxido-bridged annulenes. The geometries of these structures are summarized in the supplementary material.

Delocalized vs. Localized Annulene Structures. At the highest level of both ab inito and semiempirical theory (MP2/STO-3G and MNDO/BW plus size consistency corrections), the C_{2v}-symmetrical annulene structures **8** and **13** with a delocalized π-system are found to be more stable than the C_s-symmetrical structures **9** and **14** with highly localized double bonds (Table I). The two oxido-bridged annulenes are true Hückel aromatic systems with 10 and 14 π electrons, which is amply documented by experimental investigations carried out by Vogel and co-workers.[8] The calculated geometries of **8** and **13** are in reasonable accord with experimental geometries[17,18] (Table II).

As for the semiempirical heats of formation, the MNDO/BW values are significantly higher than the MNDO values, which is probably due to the different parametrization schemes. Since parametrization at the MNDO/BW level did not take into account size consistency corrections,[11] it is not advisable to use corrected

(12) (a) Langhoff, S. R.; Davidson, E. R. *Int. J. Quantum Chem.* **1974**, *8*, 61–65. (b) Pople, J. A.; Seeger, R.; Krishnan, R. *Int. Quantum Chem. Symp.* **1977**, *11*, 149–163.
(13) Cremer, D.; Thiel, W. *J. Comp. Chem.*, in press.
(14) STO-3G: Hehre, W. J.; Stewart, R. F.; Pople, J. A. *J. Chem. Phys.* **1969**, *51*, 2657–2664. 4-31G: Ditchfield, R.; Hehre, W. J.; Pople, J. A. *J. Chem. Phys.* **1971**, *54*, 724–728.
(15) (a) Haddon, R. C.; Raghavachari, K. *J. Am. Chem. Soc.* **1985**, *107*, 289–298. (b) Cremer, D.; Dick, B.; Christen, D. *THEOCHEM.* **1984**, *110*, 277–291.
(16) Møller, C.; Plesset, M. S. *Phys. Rev.* **1934**, *46*, 618–622.
(17) Bailey, N. A.; Mason, R. *Chem. Commun.* **1967**, 1039–1040.
(18) Ganis, P.; Dunitz, J. D. *Helv. Chim. Acta* **1967**, *50*, 2369–2378.

Table III. Theoretical Heats of Formation $\Delta H_f°$ as Obtained from MNDO Calculations[a]

molecule	symmetry	$\Delta H_f°$	$\Delta\Delta H_f°$
	1,6-Oxido[10]annulene		
9	C_s	45.7	0
10	D_{2h}	120.1	74.4
11	C_{2v}	111.9	66.2
12	C_{2v}	108.7	63.0
12′	C_{2v}	rearranges to **12**	
	1,6:8,13-Bisoxido[14]annulene		
14	C_s	47.3	0
15	C_s	86.4	39.1
15′	C_s	97.4	50.1
16	C_s	79.3	32.0
16′	C_s	81.6	34.3
17	C_s	rearranges to **16**	
17′	C_s	rearranges to **16′**	
18	D_{2h}	152.8	105.5
19	C_{2v}	133.6	86.3
20	C_{2v}	116.3	69.0
20′	C_{2v}	rearranges to **20**	
	1,6-Imino-8,13-oxido[14]annulene		
21, endo	C_s	89.4	0
21′, endo	C_s	89.4	0
21, exo	C_s	89.6	0.2
21′, exo	C_s	90.6	1.2
21, N sp^2	C_s	94.9	5.5
22, endo	C_s	126.5	37.1
22′, endo	C_s	139.5	50.1
22, exo	C_s	127.3	37.9
22′, exo	C_s	140.4	51.0
23, endo	C_s	118.5	29.1
23′, endo	C_s	122.6	33.2
23, exo	C_s	121.7	32.3
23′, exo	C_s	126.0	36.6
	1,6-Methano-8,13-oxido[14]annulene		
24	C_s	82.4	0
24′	C_s	83.1	0.7
25	C_s	118.4	36.0
25′	C_s	131.6	49.2
26	C_s	109.3	26.9
26′	C_s	115.9	33.5

[a] All values in kcal/mol. Primed structures correspond to bond-shift tautomers.

MNDO/BW $\Delta H_f°$ values. MNDO values of $\Delta H_f°$ obtained for localized structures seem to come close to experimental $\Delta H_f°$ values. This is confirmed when comparing the relevant data of 1,6-methano-, 1,6-imino-, and 1,6-oxido[10]annulenes: $\Delta H_f°$ (MNDO, localized form) = 79.5, 87.3, and 45.7 kcal/mol; $\Delta H_f°$ (experimental) = 75.2, 87.8, and 47.8 kcal/mol.[19] Therefore, we have chosen $\Delta H_f°$ (MNDO) of **9**, **14**, **21**, and **24** as appropriate reference enthalpies (Table III).

The correlation-corrected $\Delta H_f°$ values listed in Table I indicate that the relative stabilities of bond-equalized and bond-alternate structures change by 9.5 and 19.5 kcal/mol, for the 10π and the 14π annulene, respectively. These enthalpy changes can be used when assessing the degree of π-delocalization from the calculated $\Delta H_f°$ values shown in Table III.

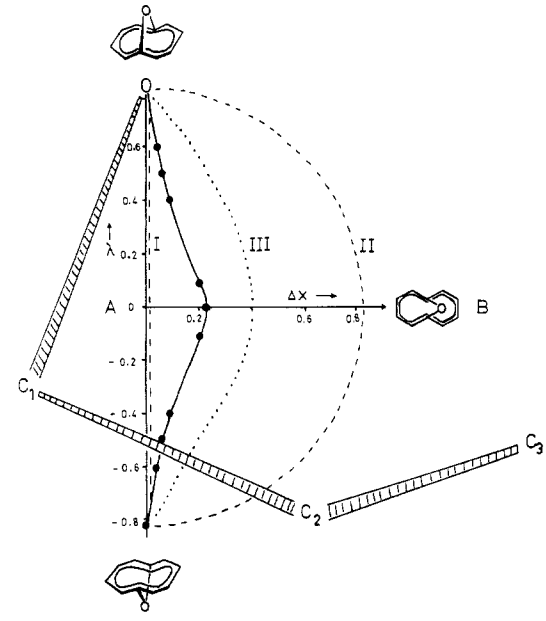

Figure 2. Trajectory of the O atom (solid line) during bridge inversion of 1,6-oxido[10]annulene. The abscissa ΔX of the coordinate system measures the deviation of the O atom from the 1,6 midpoint, the ordinate λ the height of the O atom above this point. Units are given in Å. Calculated positions of O for a fixed value of λ are indicated by dots. Dashed lines present possible trajectories for a pure inversion at the O atom (I), a pure "oxepin inversion" (II), and a combination of the two processes (III).

Table IV. Barriers to Bridge Inversion

bridge(s)	size of annulene	bridge inversion[a]	R(CC)[b]	inversion at O[a]	ΔX[c]	∠COC[d]
O	10	63.0	2.22	66.9	0.23	160.5
O, O	14	32.0	2.32; 2.32	39.1	0.31	152.9
NH, O	14	29.1	2.37; 2.34	37.1	0.33	151.6
CH_2, O	14	26.9	2.41; 2.35	36.0	0.34	150.7

[a] Calculated barriers to bridge inversion and inversion at oxygen atom in kcal/mol. [b] Distance between C1 and C6 and C8 and C13, respectively, in Å. [c] Shift of O atom out of the central position between C1 and C6 (C8 and C13) in the TS of bridge inversion given in Å. [d] COC angle in the TS of bridge inversion given in deg.

Bridge Inversion of 1,6-Oxido[10]annulene. In Figure 2 possible trajectories of the O atom (dashed lines) for its movement through the ring plane into the opposite position are shown. One can distinguish between a pure inversion at the O atom (path A in Scheme II) corresponding to trajectory I and an "oxepin inversion" (path B in Scheme II) corresponding to trajectory II. Both I and II lead to TSs (A and B, Figure 2) which are energetically highly unfavorable due to strongly deformed valence bond angles. In TS A, the COC angle is widened to 180°, while in TS B two of the four OCC angles are smaller than 90°. In order to avoid extreme angle deformations, the O trajectory may resemble III, which is an equally weighted combination of I and II.

According to our calculations the actual movement of the O atom (solid line in Figure 2) first follows trajectory I, i.e., the bridge inversion starts as an inversion at the O atom. On approaching the center of the ring, the O atom buckles sidewards. This sideward shift is calculated to be maximally 0.23 Å (Table IV and Figure 2). The COC angle widens from 106° to 160°, while two of the OCC angles narrow from 115° to 96°. The TS corresponds to structure **12**.[28] Attempts to locate the bond-shifted

(19) Bremser, W.; Hagen, R.; Heilbronner, E.; Vogel, E. *Helv. Chim. Acta* **1969**, *52*, 418–431.

(20) Pauling, L. *The Nature of the Chemical Bond*; Cornell University Press: Ithaca, NY, 1960; p 257.

(21) Klopman, G.; Andreozzi, P.; Hopfinger, A. J.; Kikuchi, O. *J. Am. Chem. Soc.* **1978**, *100*, 6267–6268.

(22) MNDO leads to an unrealistic $\Delta H_f°$ value in the case of **27** which may be due to an overestimation of steric repulsion between the bridge atoms and an underestimation of aromatic stabilization in the syn isomer.

(23) Vogel, E.; Haberland, U.; Günther, H. *Angew. Chem.* **1970**, *82*, 510–512; *Angew Chem., Int. Ed. Engl.* **1970**, *9*, 513–514.

(24) Attempts to obtain a reasonable barrier value for **27** with the aid of MNDO failed. $\Delta H_f°$* was far too high, probably because of a severe underestimation of π-electron delocalization in a strongly distorted ring framework.

(25) The TS of the successive bridge inversion contains a planar oxepandiene or oxepin unit. Therefore, it is reasonable to estimate ΔS^* from relevant values obtained for the inversion of oxepin or cycloheptatrienes: Tochtermann, W. *Top. Curr. Chem.* **1970**, *15*, 378–444.

(26) Vogel, E.; Haberland, U.; Ick, *J. Angew. Chem.* **1970**, *82*, 514–516; *Angew. Chem., Int. Ed. Engl.* **1970**, *9*, 517–518.

(27) Dewar and McKee (Dewar, M. J. S.; McKee, M. L. *Pure Appl. Chem.* **1980**, *52*, 1431–1441) have shown that when UMNDO (UHF version of MNDO) is used, bond-equalized rather than bond-alternate geometries are obtained for both normal and bridged annulenes. Unfortunately, $\Delta H_f°$ values are too low by 10–20 kcal/mol and expectation values of $\tilde{S}^2$ are much larger than 0 at the UMNDO level.

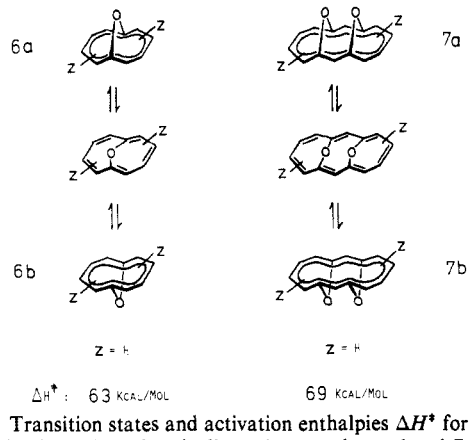

Figure 3. Transition states and activation enthalpies $\Delta H^{\ddagger}$ for (synchronous) bridge inversion of optically active annulenes **6** and **7**.

tautomer of **12**, **12'**, failed. We conclude that the structure with an oxepin unit (**12**) is electronically more favorable than the one with an oxepandiene unit (**12'**) since the latter comprises strongly distorted double bonds in the case of the [10]annulene.

The calculated activation enthalpy for bridge inversion is 63 kcal/mol. It is only 3 kcal/mol lower than the one for true inversion at O (Table III). This and the fact that the deviation of the O atom from the center of the ring is just one-fourth of the O deviation in a true "oxepin inversion" (Figure 2) suggest, to speak of, an inversion at an ether O atom.

In view of the high inversion barrier, there will be hardly any chance of observing bridge inversion for type **6** compounds. Obviously, the barrier value is a result of the small diameter and the rigidity of the [10]annulene perimeter. In the TS the 1,6 distance is widened from 2.2 to 2.6 Å, endocyclic ring angles are either compressed (CCO) or widened (CCC, COC), and in comparison to the CO bond length in **8** or planar oxepin (1.39 Å),[15b] its value (1.33 Å) is rather small in TS **12**. All these observations point to a considerable increase in strain during bridge inversion. In addition, part of the aromatic stabilization energy is lost in TS **12**. Both strain and perturbation of the 10π-system are responsible for the high barrier to inversion. A lower barrier value can only be expected if the annulene perimeter is larger and more flexible and the loss of aromatic delocalization energy less pronounced.

Bridge Inversion of 1,6:8,13-Bisoxido[14]annulene. Two basically different bridge inversion processes are possible for type **7** compounds. First, a synchronous inversion of both bridges can take place as shown in Figure 3. Possible TSs are **18–20** (Figure 1) and similar structures derived therefrom. Second, a stepwise inversion process is possible with one bridge inversion at a time and *anti*-1,6:8,13-bisoxido[14]annulene (**27**) as an intermediate (Figure 4). The synchronous passage of the O atoms through

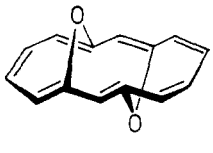

27

the ring plane is a high-energy process with $\Delta H^{\ddagger}$ = 69 kcal/mol (TS **20** Table III). Again, pure inversion at both O atoms requires even more energy (86 kcal/mol, Table III). Deviations of the O atoms from the C1,C6 and the C8,C13 midpoint are 0.37 and 0.04 Å corresponding to COC angles of 148° and 177°; i.e., the synchronous process consists of an oxepin inversion and an inversion at oxygen. Due to its high activation barrier it is unlikely to occur upon heating of type **7** compounds.

Successive bridge inversion will proceed via TS **16** or **16'**, which differ by 2 kcal/mol in energy. Despite of unfavorable electrostatic

(28) Since MNDO exaggerates bond alternation, the actual geometries of transition states and other transient forms are probably closer to a bond-equalized geometry. See also ref 27.

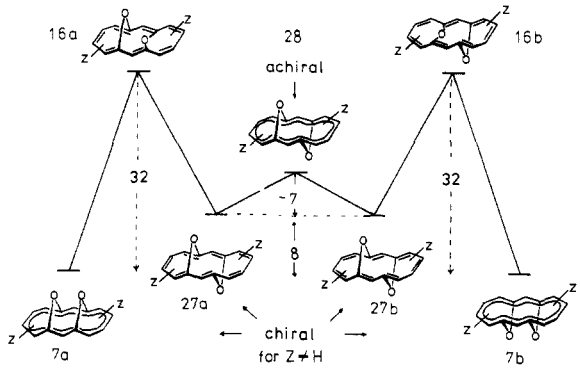

Figure 4. Mechanism of racemization for an optically active 1,6:8,13-bisoxido[14]annulene (**7**). Barriers and enthalpy differences are given in kilocalories/mole.

interactions, the first O bridge swings inwardly toward the other bridge. The latter, however, avoids a close contact with the former by an evading movement in the opposite direction. In **13** (**14**), the O,O distance is 2.60 (2.57) Å (experimental 2.55 Å, Table II). This value is only slightly reduced during the inversion process; i.e., it is always larger than the van der Waals distance between two O atoms (2.4 Å).[20] The calculated trajectory of the inverting O atom resembles the one shown in Figure 2. In TS **16** the O atom deviates by 0.31 Å from the C1,C6 midpoint. The corresponding COC angle is 153° (Table IV). Bridge inversion has lost somewhat the character of a pure inversion at O. The latter requires 7 kcal/mol more in energy (TS **15**, Tables III and IV).

Two of the eight OCC angles in **13** are compressed from 115° to 106° (**16**) and 99° (**16'**), respectively. The flipping of one O bridge in **13** leads to a less strained TS than bridge inversion in **8**. Accordingly, the corresponding barrier is 32 (34) kcal/mol (Tables III and IV), just one-half of the barrier calculated for **8**. The larger perimeter of the [14]annulene (compare also *R* values in Table IV) facilitates the inversion process.

It is interesting to note that the calculated barrier is within a few kilocalories/mole of the barrier to linearization for H_2O (37 kcal/mol).[4] This coincidence, however, can only be accidental since different effects determine the magnitude of the two barriers. For H_2O, it is mainly the increase in energy of the $3a_1$ MO converting to the $1\pi_u$ MO, which determines the height of the barrier. In **16** this increase will be less significant since a linear arrangement of the CO bonds is not realized and partial delocalization of the $2p\pi$(O)-electrons is possible. The actual height of the barrier is predominantly due to increased strain in the annulene perimeter and a partial loss of aromatic stabilization of the 14π-system.[28]

Bridge Inversion of 1,6-Imino-8,13-oxido[14]annulene (21) and 1,6-Methano-8,13-oxido[14]annulene (24). Since the barrier to bridge inversion is sensitive to the size of the annulene perimeter, enlargement of the 1,6 and 8,13 distances should lead to a further decrease of the barrier value. The 1,6 (8,13) distance depends on the nature of the bridge atom. Replacement of one oxido bridge in **13** by an imino or a methano bridge (compounds **21** and **24** in Figure 1) should widen the [14]annulene perimeter, since the CX bond length increases for X = O, N, and C from 1.385 to 1.446 (**21**) and 1.522 Å (**24**), thus keeping C1 and C6 further apart than in **13** (Table IV).

Oxido-bridge inversion of **21** and **24** proceeds via TSs **23** and **26**,[28] respectively. The calculated barrier values are 29 and 27 kcal/mol (Table IV). An enlargement of the perimeter by replacement of one oxido bridge in **13** reduces the barrier by 3 and 5 kcal/mol. Steric repulsion between the bridge atoms may also contribute to a decrease in the inversion barriers by destabilizing the syn configuration relative to the TS of the inversion process. This at least is suggested by the geometries of **21** and **24** which reveal that the NH and CH_2 bridge are bent away from the oxido bridge by about 10°, thus leading to additional distortion of the annulene perimeter. A similar but less pronounced reduction is evaluated for the barriers to inversion at O (Table IV). The deviation ΔX of the O atom from the C8,C13 midpoint in the TSs

23 and **26** increases, and the COC angle decreases slightly in the series **16**, **23**, and **26** (Table IV).

For **21**, two orientations of the NH bond are possible, namely endo, directed toward the neighboring O bridge, and exo, outwardly directed away from the oxido bridge. Clearly, the former conformation is more stable due to H bonding with the O atom. Modified NDO methods are known to underestimate the stability of H bonding,[21] and therefore, the enthalpy difference of 1 kcal/mol calculated in this work (Table III) is probably only a lower bound to the true value. On the other hand, one has to keep in mind that pyramidalization at N is better realized for the exo form (∠(C1C6)NH = 127.8°) than for the endo form (∠(C1C6)NH = 133.7°) since the vicinity of the O atom hinders a further inward bending of the NH bond. Accordingly, the calculated barrier to inversion about the N atom is just 5.5 kcal/mol (Table III).

One might argue that oxido-bridge inversion in **21** requires a lower energy if the NH bond is exo oriented. The calculated $\Delta\Delta H_f°$ values (Table III) show that this is not the fact. Attractive interactions between H and O clearly stabilize the endo form of TS **23**.

Mechanism of the Racemization of Optically Active Bridged Annulenes. Recently, 2,7-Br_2-**6** and 2,9-Br_2-**7** have been quantitatively separated into their enantiomers by chromatography on triacetylcellulose.[9] Upon heating, **6** turned out to be optically stable up to 250° C. Since racemization of **6** must involve inversion of the oxido bridge, it was concluded that the inversion barrier of **6** is higher than 42 kcal/mol.[9b] This is in line with the MNDO barrier of 63 kcal/mol calculated for the parent annulene (Table IV).

In contrast to the [10]annulene, **7** racemizes above 120 °C. A racemization barrier of $\Delta G^{\ddagger}$ = 32 kcal/mol has been determined.[9a] On the basis of the calculations carried out in this work, we suggest the following racemization mechanism (compare with Figure 4). The enantiomer **7a** rearranges via bridge inversion to **27a**. **27a** is also chiral. It possesses a strongly distorted 14π perimeter, with CCCC dihedral angles deviating maximally by 60° from the ideal values in a planar ring framework (Table II). As a consequence, π-conjugation is disturbed and **27** possesses alternating bonds. At the HF/STO-3G level of theory, **27** is 8 kcal/mol higher in energy than the syn isomer of the [14]annulene.[22] Assuming a ΔG value of similar magnitude, there is less than 0.1% **27** in the equilibrium mixture at 120 °C. This means that attempts to detect **27** by rapid cooling of the equilibrium mixture will be difficult because of the small amount of **27** formed.

If the second bridge of **27a** (Figure 4) inverts, TS **16'** will be traversed, which is 2 kcal/mol higher in energy than TS **16**. An energetically more favorable reaction path is shown in Figure 4. **27a** can convert by π-bond shift via **28** (Figure 4) to **27b**. The barrier of this process has been measured to be close to 7 kcal/mol in the case of *anti*-1,6:8,13-bismethano[14]annulene.[23,24] The molecule can easily surmount this barrier, since it possesses an excess energy of about 24 kcal/mol once the barrier to bridge inversion has been crossed. Enantiomer **27b** is formed which possesses the correct double bond arrangement for an isomerization via TS **16b** to **7b**.

The rate of racemization depends on the rate constants of five equilibria:

$$\mathbf{7a} \underset{k_{-1}}{\overset{k_1}{\rightleftharpoons}} \mathbf{27a} \qquad \mathbf{7b} \underset{k_{-1}}{\overset{k_1}{\rightleftharpoons}} \mathbf{27b}$$

$$\mathbf{7a} \underset{k_{-2}}{\overset{k_2}{\rightleftharpoons}} \mathbf{27b} \qquad \mathbf{7b} \underset{k_{-2}}{\overset{k_2}{\rightleftharpoons}} \mathbf{27a}$$

$$\mathbf{27a} \underset{}{\overset{k_3}{\rightleftharpoons}} \mathbf{27b}$$

Considering the enthalpy differences shown in Figure 4, we can predict that (1) both concentration and concentrational changes of **27** are vanishingly small, (2) $k_1 > k_2$ ($k_{-1} > k_{-2}$), and (3) $k_3 \gg k_{-1}$ ($k_3 \gg k_{-2}$). Accordingly, the rate of racemization (R) is given by the rate of bridge inversion (I)

$$k_R = k_I = k_1 + k_2 \approx k_1$$

in other words $\Delta G_I^{\ddagger}$ can be determined by measuring $\Delta G_R^{\ddagger}$. If one assumes an activation entropy $\Delta S^{\ddagger} \geq -5$ cal/(K mol)[25] for the stepwise inversion process, then the calculated $\Delta H^{\ddagger}$ value will lead to a theoretical $\Delta G^{\ddagger}$ of 32–34 kcal/mol, which is in accord with the experimental barrier to racemization of 2,9-Br_2-**7**. We conclude that the racemization mechanism comprises a successive inversion of the bridges, the intermediacy of **27**, and a π-bond shift from **27a** to **27b**.[29]

How To Measure Bridge Inversion in 21 and 24? In order to verify the calculated decrease in the inversion barrier when replacing one oxido bridge in **13** by a NH or CH_2 bridge, one could think or synthesizing optically active derivatives of **21** and **24** and investigating their racemization rates. We predict that racemization of these compounds will not occur, since an inversion of the imino or methano bridge, necessary for a configurational change similar to **7a** → **7b** (Figure 4), requires more than 50 (**21**) and 100 kcal/mol (**24**). *Chiral derivatives of **21** and **24** will be optically stable.*

Another possibility of measuring the barrier to oxido-bridge inversion would be given, if the concentration of *anti*-1,6-imino-8,13-oxido[14]annulene (**29**) and *anti*-1,6-methano-8,13-oxido-[14]annulene (**30**) becomes large enough for spectroscopic detection upon heating of **21** and **24**, respectively. Although MNDO leads to unreasonable $\Delta H_f°$ values for the anti isomers,[22] a thorough analysis of relative enthalpies suggests that the anti isomers **29** and **30** should be up to 4 kcal/mol more stable than **27** in relation to the corresponding syn configurated annulenes. **24** has been synthesized by Vogel and co-workers.[26] However, no specific search for its anti isomer has been carried out so far.

A possible way of increasing the concentration of **30** would be to destabilize syn isomer **24**. For example, appropriate substituents at the bridge carbon would lead to steric repulsion in **24**. Hence, formation of the anti isomer should be facilitated. We suggest the synthesis of **31** along the lines described by Vogel for **24**.[26]

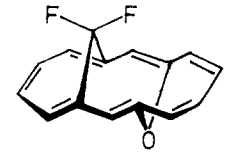

31

Alternatively, one could investigate derivatives of **24**, with CHR bridges. A bulky alkyl substituent will be exo positioned with regard to the second bridge. Its steric interactions with the annulene perimeter will force the CHR bridge to move toward the oxido bridge, thus destabilizing the syn isomer and increasing the chance of detecting the anti form **30**. If the concentration of the latter could be measured as a function of T, then an experimental determination of both $\Delta\Delta G$ (syn–anti) and $\Delta G_I^{\ddagger}$ for **24** would be possible.

Conclusions

(1) Oxido-bridged [10]annulenes do not undergo, [14]annulenes do undergo, bridge inversion upon heating. The barrier height depends critically on the size of the annulene perimeter. We predict barrier values of 32, 29, and 27 kcal/mol for **13**, **21**, and **24**, respectively.

(2) Bridge inversion is predominantly an inversion at the ether atom, the first which has been observed so far.[6] The COC angle is widened to 150° in the TS of the inversion process.

(3) The mechanism of the racemization of optically active **7** is shown in Figure 4. It involves successive rather than synchronous inversion of the O bridges. **27** is formed as an intermediate. It is 8 kcal/mol less stable than the syn configuration and possesses an bond-alternate form. Rearrangement to the valence tautomeric form by a π-bond shift is a fast process. A kinetic analysis based on the enthalpy differences calculated in

(29) The intermediacy of any norcaradienic form can be ruled out since shortening of the 1,6 and/or 8,13 distance leads to a significant decrease of the perimeter size and, hence, to suppression of bridge inversion.

this work yields $k_I = k_R$ and, hence, $\Delta G_I^{\ddagger} = \Delta G_R^{\ddagger}$.

(4) We predict that the anti form **30** can be experimentally detected if appropriate substituents are incorporated at the CH_2 bridge.

Acknowledgment. Fruitful discussions with Prof. E. Vogel and Prof. K. Schlögl are acknowledged. This work was supported by the Deutsche Forschungsgemeinschaft and the Fonds der Chemischen Industrie. Calculations have been carried out at the Rechenzentrum der Universität Köln and at the Computation Center of the Philadelphia College of Textiles & Science.

Registry No. 6b, 102807-83-0; **7b**, 102916-53-0; **9**, 4759-11-9; **14**, 102916-52-9; **21**, 102807-82-9; **24**, 29918-22-7.

Supplementary Material Available: Three tables containing geometries of **10–12** and **15–26** (4 pages). Ordering information is given on any current masthead page.

Ab Initio Studies of Molecular Structures and Energetics. 1. Base-Catalyzed Hydrolysis of Simple Formates and Structurally Related Reactions

Carl S. Ewig* and John R. Van Wazer

Contribution from the Department of Chemistry, Vanderbilt University, Nashville, Tennessee 37235. *Received December 16, 1985*

Abstract: Molecular structures, conformations, and thermodynamic properties of the orthoformate anionic molecules produced by the interaction of hydroxy or methoxy ions with formic acid or methyl formate have been determined by ab initio computations. These substances are the accepted intermediates, or models thereof, in the hydrolysis of esters, both in basic solution and by enzymes. The simplest of these orthoformate ions—$[HCO(OH)_2]^-$, formed from formic acid and a hydroxyl ion—and some related compounds were examined in a series of good-quality basis sets and, like the other orthoformates studied, were proven to be stable compounds rather than transition-state molecules. Energies were computed at the SCF and MP2 levels of approximation, with and without addition of diffuse basis functions. Theoretical corrections for nuclear motion were computed and used to obtain values of ΔH°_{298} for a series of reactions including the postulated steps in base-catalyzed and enzymatic hydrolyses. The stable conformers were found to correspond to the hydrogen of an OH (or OCH_3) group being adjacent or opposed to the lone oxygen, with both adjacent being the more stable. A modified Fourier expansion of the OH and OCH_3 torsional potentials indicated that the conformers of the $[HCO(OH)_2]^-$ and $[HCO(OH)(OCH_3)]^-$ structures are stabilized by monopolar electrostatic forces rather than by stereoelectronic effects.

Recent rapid advances in computational techniques and resources have made possible the application of rigorous ab initio theoretical methods to the study of an ever-widening array of fundamental chemical problems. The ab initio approach, which is thus currently supplanting the simpler approximate ones, has the important property that no prior experimental data is required in its implementation, making it a practical and reliable tool especially suited for interesting compounds that are difficult to isolate. Of course the history of wildly unreliable quantum calculations makes it obligatory for the present-day investigator to demonstrate that his approach is as appropriate for little-known structures as it is for well-characterized, related molecules. This may be done by comparison with experiment and, by employing an often overlooked feature of the ab initio approach, the intercomparison of results computed at various levels of approximation.[1] The study presented here, dealing with anions of organic orthoacids and esters—structures that have been widely invoked as intermediates in ester hydrolysis—is a particularly useful example of both these aspects of the ab initio method and philosophy.

From the interpretation of kinetic experiments and other experimental data, the base-catalyzed hydrolysis of organic esters and peptides has been shown to involve an orthoacid derivative (a monoesterified orthoacid anion, $[R'CO(OR)(OH)]^-$, for ester hydrolysis) produced by nucleophilic attack on the carbonyl carbon atom. Because the tricoordinated carbonyl carbon atom of the ester becomes tetracoordinated in its orthoacid derivative, the latter is sometimes called a "tetrahedral intermediate" and is usually assumed to be thermodynamically less stable than its precursors or successors in the hydrolysis process.

Enzymatic hydrolyses of esters also appear to proceed through such intermediate structures.[2] Thus, hydrolytic enzymes such as the serine esterases and proteases exhibit a strongly basic group (i.e., a serine residue) which is considered to act as a substituent in a "tetrahedral intermediate". Another such intermediate is involved in a subsequent step in which water is taken up prior to disengagement of the substrate. In one or both steps the enzyme is believed to exhibit a topology that maximizes its binding to several sites in the intermediate. Hence knowledge of the molecular structure of these intermediates provides indirect (template) information about the enzyme active site and the structural requirements for binding to the site by other compounds, such as inhibitors.

Gas-phase reactions between esters and strong bases have been the subject of detailed experimental studies[3-5] employing mass spectroscopy and ion-cyclotron resonance. To date these have provided no direct evidence of the existence of tetrahedral intermediates. In fact it has recently been suggested, based on this type of data, that these tetracoordinate intermediates are not even stable species in the gas phase but rather transition states.[4] Also there is apparently no experimental information about their structural parameters.

Some prior theoretical investigations have been reported concerning the structure and properties of this type of intermediate species. These fall into two groups: (a) early studies[6,7]—employing

(1) For a comprehensive review, see: Hehre, W. J.; Radom, L.; Schleyer, P. *Ab Initio Molecular Orbital Theory*; Wiley: New York, 1986.

(2) For example, see: Kraut, J. *Annu. Rev. Biochem.* **1977**, *46*, 331-358.
(3) Smit, A. L. C.; Field, F. H. *J. Am. Chem. Soc.* **1977**, *99*, 6471-6483.
(4) Takashima, K.; Josē, S. M.; Amaral, A. T. d.; Riveros, J. M. *J. Chem. Soc., Chem. Commun.* **1983**, 1255-1256.
(5) Johlman, C. L.; Wilkins, C. L. *J. Am. Chem. Soc.* **1985**, *107*, 327-332.

0002-7863/86/1508-4774$01.50/0